Clays and Clay Minerals, Vol. 57, No. 3, 371–382, 2009.

APPLICATION OF CHEMICAL GEOTHERMOMETRY TO LOW-TEMPERATURE TRIOCTAHEDRAL CHLORITES

Atsuyuki Inoue*,†, Alain Meunier, Patricia Patrier-Mas, Cecile Rigault, Daniel Beaufort, and Philippe Vieillard

Laboratoire Hydr'ASA, UMR 6532 CNRS, Université de Poitiers, 40 avenue du Recteur Pineau, 86022 Poitiers Cedex, France

Abstract—Low-temperature chlorites formed in diagenetic to low-grade metamorphic environments generally have greater Si contents and larger numbers of octahedral vacancies, and smaller Fe+Mg contents than higher-grade metamorphic chlorites. The compositional variations are characterized approximately by four end-member components: Al-free trioctahedral chlorite, chamosite, corundophilite, and sudoite. The solid solution is considered to be a random mix of cations and vacancies in the octahedral sites. Using the compositions of chlorites from Niger, Rouez, and Saint Martin diagenetic-hydrothermal series, a new, more convenient geothermometer, applicable to low-T chlorites is proposed and comparison made with geothermometers proposed previously. The chlorites studied contain appreciable amounts of Fe(III) (>14% of the total Fe), determined by Mössbauer spectroscopy. The calculations under which all Fe was regarded as ferrous gave considerable overestimates for the formation temperature, irrespective of the geothermometer used. This problem was reduced by taking into account the presence of Fe(III) in the octahedral sites. The geothermometer from this study gave more reasonable estimates than the geothermometers proposed by Walshe (1986) and Vidal *et al.* (2001), particularly in the case of the Niger chlorites which crystallized in the lowest-temperature conditions. The ordered-site substitution model of solid solution developed by Vidal *et al.* (2001) predicted satisfactorily the formation temperature of the Rouez chlorites and of some of the Saint Martin chlorites, suggesting that the chlorite compositions are controlled by the $\mathrm{Si}\square R^{2+}_{-2}$ exchange at low-T conditions while they are controlled by Tschermak exchange at higher temperatures. The decreasing number of vacancies with temperature are poorer in Fe-rich than in Fe-poor chlorites. Furthermore, the ordered-site occupation of cations and vacancies in trioctahedral chlorite occurs concomitantly with the compositional changes ruled by increasing temperature conditions.

Key Words—Chlorite, Diagenesis, Ferric Iron, Geothermometry, Hydrothermal Alteration, Low-grade Metamorphism, Mössbauer Spectroscopy, Solid Solution.

INTRODUCTION

Chlorite is a common rock-forming mineral found in a variety of geologic environments including diagenetic, low- to high-grade metamorphic, and hydrothermally altered rocks with different bulk-rock compositions (Laird, 1988). Chlorite displays a wide range of non-stoichiometric compositional variations depending on bulk-rock composition and the physicochemical conditions which prevailed at the time of formation, including temperature (T), pressure (P), pH, and the activities of various metal cations dissolved in fluid, together with the activities of S_2, O_2, and CO_2. The variation in chemical composition of chlorite is a useful source of information on the physicochemical conditions of formation; the use of chlorite composition in estimating the formation temperature is referred to as 'chemical chlorite geothermometry'. Another type of geothermometry for chlorite, related to the polytype structure (Hayes, 1970; Walker, 1993), is not considered here.

As summarized by Vidal *et al.* (2001), two approaches to chemical geothermometry have been proposed: (1) empirical calibrations based on the tetrahedral Al (hereafter abbreviated as ^{IV}Al) occupancy and/or the octahedral vacancy as a function of measured temperatures in active geothermal systems and homogenization temperatures of fluid inclusions in fossil geothermal systems; and (2) thermodynamic calculation of equilibrium conditions for chlorites, the composition of which is expressed as the activities of end-member components of known thermodynamic properties. The first approach has been applied to diagenetic, low-grade metamorphic chlorites because of its simplicity. However, many previous studies indicated that chlorite compositions are sensitive not only to prevailing physicochemical conditions but also to bulk-rock composition (*e.g.* De Caritat *et al.*, 1993; Zane *et al.*, 1998). Although various equations based on different rock compositions have been proposed, none has given reliable results over a wide range of physicochemical conditions of formation (De Caritat *et al.*, 1993; Vidal *et al.*, 2001).

Many advantages are found in the second, thermodynamics-based geothermometer. In addition to the estimation of formation temperature and pressure, it takes into account the variations of the rock mineralogy,

---

* E-mail address of corresponding author:
atsuyuki_inoue@faculty.chiba-u.jp
† Permanent address: Department of Earth Sciences, Chiba University, Chiba 263-8522, Japan
DOI: 10.1346/CCMN.2009.0570309

including elemental partitioning between coexisting minerals (*e.g.* Vidal *et al.*, 2001) and the potential influence of additional physicochemical parameters such as fluid composition and redox conditions (Walshe and Solomon, 1981; Walshe, 1986). De Caritat *et al.* (1993) tested the validity of two thermodynamic geothermometries developed by Walshe (1986) and Hutcheon (1990), and concluded that no single chlorite geothermometer performs satisfactorily over the whole range of natural conditions, probably resulting from uncertainties in the thermodynamic properties of chlorites used and from the unsuitable mixing model for chlorite solid solution used in these studies. De Caritat *et al.* (1993) ignored the effect of Fe(III) contents in estimating the formation temperature. Following criticism of the De Caritat *et al.* (1993) work, many researchers carried out experimental and theoretical studies in an effort to revise the thermodynamic properties of chlorites and to apply them to experimental or natural systems (*e.g.* Berman, 1988; Saccocia and Seyfried, 1994; Baker and Holland, 1996; Holland and Powell, 1998; Holland *et al.*, 1998; Vidal *et al.*, 1992, 1999, 2001, 2005; Parra *et al.*, 2005). Although the previous studies were largely carried out on higher-grade metamorphic chlorites, that by Vidal *et al.* (2001) may be noteworthy in terms of the geothermometry applicable to low-*T* chlorites. Those authors proposed a thermodynamic model for Fe-Mg partitioning of aluminous trioctahedral chlorites applicable to a wide range of *T* (100–600ºC) and *P* (1–25 kbar) conditions by calibrating data from phase-equilibrium experiments and natural mineral assemblages.

Foster (1962) indicated that the Fe(III) contents of metamorphic chlorites were <4% of the total Fe and thereafter, the presence of Fe(III) was usually ignored in the structural formula calculations of higher-grade metamorphic chlorites because the ferric/ferrous ratio cannot be determined by microprobe analysis. However, this assumption has not been verified to be commonly applicable to low-*T* chlorites. Because significant amounts of Fe(III) strongly influence the number of vacancies in the chlorite structure (Laird, 1988), Fe(III) should be taken into consideration when estimating the temperature of formation. Because the low-*T* chlorites display different features of compositional variations from those of higher-grade metamorphic chlorites (Curtis *et al.*, 1985; Hillier and Velde, 1991), the validity of the geothermometer proposed by Walshe (1986) and Vidal *et al.* (2001) for low-*T* chlorites formed under diagenetic to very low-grade metamorphic conditions needs to be verified.

The present work is an extension of the work of De Caritat *et al.* (1993) and of Hillier and Velde (1991). The validity of the geothermometers proposed by Walshe (1986) and Vidal *et al.* (2001) was tested using new analytical data of chlorites from three locations, Niger, Rouez, and Saint Martin. The data set contains the proportions of Fe(III) determined independently by Mössbauer spectroscopy. Particular emphasis in this study was placed on evaluation of the effect of Fe(III) on the estimate of temperature of formation. The goal was to develop another, more convenient geothermometer, which can be used for diagenetic, very low-grade metamorphic chlorites. The geothermometer based on the chlorite-carbonate equilibria, developed by Hutcheon (1990), was not considered here as that method requires compositional data from coexisting carbonates and such data are rare.

SOURCES OF ANALYSES AND GEOLOGIC SETTINGS

Niger chlorites

These samples are from sandstones of Niger, Africa (the details of location and geologic age are confidential). The chlorites were separated by a density fractionation technique using sodium polytungstate as a heavy liquid (density = 2.67 g/cm^3). The chlorites were analyzed by X-ray powder diffraction (XRD), scanning electron microscopy energy-dispersive microanalysis (SEM-EDS), and Mössbauer spectroscopy. The chlorites occur as grain-coatings of sandstones and show a rosette-like morphology, 5–10 μm in diameter. Examination by XRD showed that the chlorites contain chlorite-berthierine mixed-layer minerals. The clay mineralogy consists of abundant kaolin (kaolinite ± dickite) and minor illite. Mixed-layer illite-smectite minerals having >45% illite layers are also present in some samples. They are associated with pyrite, ankerite, and calcite. Precise data on the formation temperature are not available so ~80ºC was estimated based on the mineral association. 120 analyses were selected from the analyzed data after taking into account the Na+K+Ca contents, which are probably due to impurities and/or interstratification with smectite (Hillier and Velde, 1991). Analyses with excess SiO_2 content due to quartz contamination were disregarded. The Si contents ranged from 2.87 to 3.30 and the vacancies from 0.33 to 0.83 per half structural formula unit (p.h.f.u.) (O = 14), based on the assumption that all Fe is regarded as ferrous. The mean Fe(II)/(Fe(II)+Mg) ratio was 0.59, ranging from 0.30 to 0.80. The Fe(III) proportions were 22–34% of total Fe, determined by the Mössbauer method described by Beaufort *et al.* (1992). The Mössbauer spectra of chlorites were recorded using the powder samples separated from rocks. The Fe(III) content is probably heterogeneous between different chlorite grains present in a thin section and the values presented represent only an average.

Rouez chlorites

These chlorites are from the Brioverien (Late Precambrian) metasediments of the Massif Armorican series which surround the massive sulfide deposit near Rouez (Beaufort, 1986, 1987; Hillier and Velde, 1991).

The rocks are pelites and metagreywackes metamorphosed under lower-greenschist-facies conditions in the Hercynian orogeny, producing a clay mineral assemblage that is essentially illite + chlorite. No precise paleotemperature data for the formation of chlorite are available; they probably range from 200 to 350ºC according to the mineral assemblages without biotite. Chlorite occurring in the sulfide deposit displays a systematic variation of the Fe/Mg ratios according to the different associated minerals (Beaufort, 1986). Sixty four of the Beaufort (1986) analyses were used in this study. The Si contents ranged from 2.60 to 2.94 and the vacancies from 0.03 to 0.42 p.h.f.u., based on the assumption that all Fe is regarded as ferrous. The mean value of Fe(II)/(Fe(II)+Mg) was 0.66, ranging from 0.59 to 0.75. The Fe(III) proportions were 14–24% of total Fe by Mössbauer measurements (Beaufort, 1986). A single, average Fe(III) value was applied to the structure formula calculations of chlorites analyzed in a thin section.

Saint Martin chlorites

These chlorites are from thermally metamorphosed volcaniclastic rocks surrounding Early Oligocene quartz diorite intrusive rocks in Saint Martin, Lesser Antilles (Beaufort *et al*., 1990, 1992). Five alteration zones with different mineral assemblages surrounding the intrusion were identified. From closest to the periphery, zone 1: epidote + actinolite + magnetite; zone 2: epidote + chlorite; zone 3: epidote + chlorite + hematite; zone 4 as local veins: chlorite + phengite + magnetite; and zone 5: interstratified chlorite-smectite and illite-smectite + calcite. The chlorites used in this study are from zones 2, 3, and 4 and the paleotemperatures determined by fluid-inclusion studies are within a range of 220 to 340ºC (Patrier *et al*., 1990; Beaufort *et al*., 1992). The Si contents ranged from 2.79 to 3.04 and the vacancies from 0.05 to 0.20 p.h.f.u. in 18 analyses, based on the assumption that all Fe is regarded as ferrous. The mean values of the Fe(II)/(Fe(II)+Mg) ratios were 0.41, 0.21, and 0.58 for chlorites from zones 2, 3, and 4 respectively. The Fe(III) contents varied according to the different mineral assemblages, 25–30%, 32%, and 16% for chlorites of zones 2, 3, and 4, respectively, by Mössbauer measurements (Beaufort *et al*., 1992). This suggests that the chlorite composition was affected not only by the temperature but also by the oxygen fugacity.

COMPOSITIONAL VARIATIONS, CHOICE OF END-MEMBERS, AND ACTIVITY MODEL

Before choosing the end-member components for the chlorite solid solution and constructing the activity model, the compositional variations of the low-*T* chlorites compared to higher-grade metamorphic chlorites must be characterized. The compositions of chlorites in the R^{2+}-Si diagram presented by Wiewióra and Weiss (1990) are shown (Figures 1, 2): R^{2+} represents the octahedral cations (Mg + Fe(II) + Mn(II)). The values of R^{2+} and Si are based on O = 28. The Al-free trioctahedral chlorite pole is a fictive 14 Å chlorite component having a serpentine composition. The pyrophyllite-gibbsite is also a fictive chlorite component having a kaolinite composition. The term corundophilite is used instead of amesite because amesite is a 7 Å phase.

The data for higher-grade metamorphic chlorites obtained from Foster (1962) and Laird (1988) were plotted (Figure 1) together with the compositions of di-trioctahedral sudoite (Newman and Brown, 1987) for comparison. Most of the metamorphic chlorite compositions concentrate between the clinochlore and the

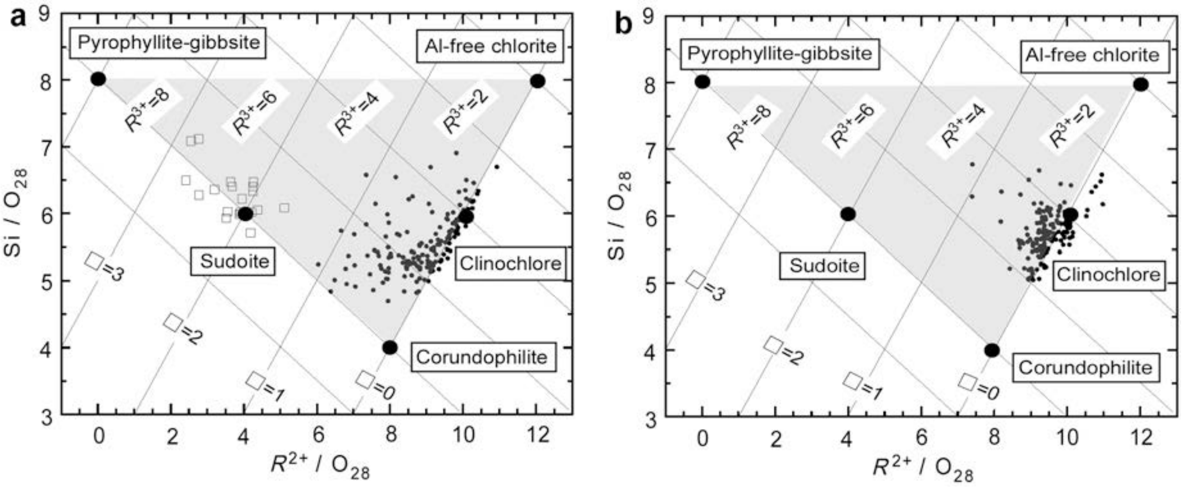

Figure 1. Chemical compositions of metamorphic chlorites plotted in the R^{2+}-Si diagram of Wiewióra and Weiss (1990): (a) chemical analyses determined by the weighing method, distinguishing Fe(III) from Fe(II) (Foster, 1962) and sudoite (Newman and Brown, 1987); (b) chemical analyses using EMPA (Laird, 1988), all Fe as Fe(II).

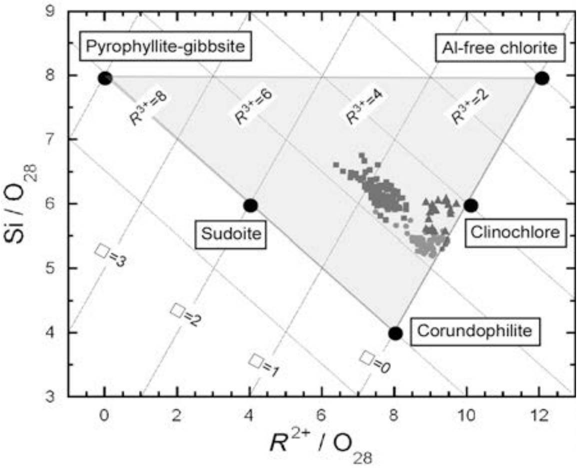

Figure 2. Chemical compositions of low-temperature chlorites from Niger (squares), Rouez (circles), and Saint Martin (triangles) plotted in the R^{2+}-Si diagram of Wiewióra and Weiss (1990); all Fe is regarded as Fe(II).

corundophilite, though some extension was observed toward the Al-free chlorite. Compared to higher-grade metamorphic chlorites, low-*T* chlorites exhibit a remarkable deviation from the Al-free chlorite and corundophilite line (Figure 2). Hillier and Velde (1991) noted that the deviation is characterized by a $\mathrm{Si}\square R^{2+}_{-2}$ exchange rather than an $^{\mathrm{VI}}\mathrm{Al}_2\square R^{2+}_{-3}$ one because the compositions of samples from a single location tend to expand nearly parallel to the line of a constant R^{3+} value, where □ denotes the octahedral vacancy. Hillier and Velde (1991) also noted a broad correlation between the number of vacancies and the Fe(III) contents. However, the number of vacancies depends on how the normalization of the chemical analyses to the structure formula has been performed (Laird, 1988).

In order to describe the complicated substitutions of chlorites mentioned above, choosing appropriate end-member components is necessary. Vidal *et al.* (2001) focused only on the substitution of chlorites with Si < 3 p.h.f.u. (O = 14) for simplicity and chose four end-members, clinochlore $[\mathrm{Mg_5Al}][\mathrm{Si_3Al}]\mathrm{O_{10}(OH)_8}$, chamosite (daphnite) $[\mathrm{Fe^{2+}_5Al}][\mathrm{Si_3Al}]\mathrm{O_{10}(OH)_8}$, corundophilite $[\mathrm{Mg_4Al_2}][\mathrm{Si_2Al_2}]\mathrm{O_{10}(OH)_8}$, and sudoite $[\mathrm{Mg_2Al_3}\square][\mathrm{Si_3Al}]\mathrm{O_{10}(OH)_8}$. The choice of the four components allows description of the Fe-Mg ($\mathrm{FeMg_{-1}}$), Tschermak ($^{\mathrm{VI}}\mathrm{Al}^{\mathrm{IV}}\mathrm{AlSi_{-1}}R^{2+}_{-1}$), and dioctahedral-trioctahedral ($\mathrm{Si}\square R^{2+}_{-2}$ or $^{\mathrm{VI}}\mathrm{Al_2}\square R^{2+}_{-3}$) substitutions occurring in trioctahedral chlorites. However, clearly the composition space adopted by Vidal *et al.* (2001) excludes many of the compositions of diagenetic chlorites (Figure 2). On the other hand, Walshe (1986) chose four framework end-members, C1: Al-free chlorite $[\mathrm{Mg_6}][\mathrm{Si_4}]\mathrm{O_{10}(OH)_8}$, C2: clinochlore, C3: chamosite, and C5: pyrophyllite-gibbsite $[\mathrm{Al_4}\square_2][\mathrm{Si_4}]\mathrm{O_{10}(OH)_8}$. The composition space of Walshe (1986) also excludes many compositions of low-*T* chlorites (Figure 2) due to the omission of the corundophilite component. As a result, the calculation of Walshe (1986) has a disadvantage: negative mole fraction values of the Al-free chlorite component in the solid solution must be dealt with. In order to avoid the problem, alternative end-members are preferred: Al-free chlorite, corundophilite, chamosite, and sudoite or pyrophyllite-gibbsite. As an alternative for sudoite or pyrophyllite-gibbsite (kaolinite composition) for the vacancy-bearing component, the vacancies in low-*T* chlorites are <2 p.f.u. (O = 28) and the composition plane delineated by the poles of Al-free chlorite, corundophilite, and sudoite covers satisfactorily almost all the plots of low-*T* chlorite compositions (Figure 2). From this line of evidence, choosing the sudoite component is reasonable in order to describe the vacancies in trioctahedral chlorites.

Knowledge of the crystal chemistry of chlorite is required to set up the ideal activity because geothermometry depends on the activity model used. The ideal structure of the trioctahedral chlorite is a regular alternation of a basic talc (or TOT) layer and a brucite (or interlayer octahedral) layer. According to Bailey (1988), the basic layers of type II*b* chlorite have different types of sites, represented as: talc layer $\{M1(M2)_2[(T1)_2(T2)_2]\mathrm{O_{10}(OH)_2}\}$ and brucite sheet $\{(M3)_2M4(\mathrm{OH})_6\}$, respectively. These sites show different preferences for cations. Based on the site preference of cations in trioctahedral chlorite, Vidal *et al.* (2001) assumed that octahedral Al is restricted to the *M*1 and *M*4 sites with a strong preference for *M*4, and tetrahedral Al is restricted to *T*2 sites where it substitutes randomly for Si. In addition, vacancies in sudoite were assumed to be restricted to the *M*1 site, while Fe, Mg, and Al mix randomly over the *M*2 and *M*3 sites, and the Mg/Fe ratio was assumed to be equal in the two sites *M*1 and (*M*2+*M*3). Fe(III), if it exists, is cast into the *M*4 site (Vidal *et al.*, 2005). As listed in Table 1, the ideal activities (a^{ideal}) of end-member components in the chlorite solid solution were calculated following the mixing on sites model (Helgeson *et al.*, 1978; Powell, 1978) based on the above ordered-substitution model.

$$a_i^{\mathrm{ideal}} = \mathrm{k}_i \prod_s \prod_j X_{j,s}^{\nu_{s,j,i}}$$

$$X_{j,s} = \frac{n_{j,s}}{\sum_j n_{j,s}} \qquad (1)$$

$$\mathrm{k}_i = \prod_s \prod_j \left(\frac{\nu_{s,j,i}}{\nu_{s,i}}\right)^{-\nu_{s,j,i}}$$

where $X_{j,s}$ is the mole fraction of the *j* cation on the *s* site, $\mathrm{k_i}$ is the normalization constant, and ν_i is the number of *s* sites. Walshe (1986) distinguished the two *T* sites of the TOT layer but not the octahedral *M* sites, assuming a random mixing of cations and vacancies between the six identical octahedral M sites. The ideal activities were also calculated on the basis of the mixing on sites model (Table 1). For the present activity calculations, an assumption was made that all Fe(III) occupies the same octahedral sites as Al. Similar to the Walshe's model (1986), a random mixing model of cations and vacancies in the six octahedral M sites was adopted in order to describe the compositional variations of low-T chlorites using the four, new end-member components defined above. The ideal activities calculated by equation 1 are listed in Table 1.

ESTIMATION OF FORMATION TEMPERATURE USING DIFFERENT GEOTHERMOMETERS

Walshe (1986) geothermometer

Walshe (1986) considered that the composition of chlorite crystallizing in equilibrium with quartz must be controlled by the fluid composition in addition to temperature and pressure. The formation reaction is expressed by the following two reactions which are independent of $a_{\mathrm{Al^{3+}}}/(a_{\mathrm{H^+}})^3$ in fluid:

$$6Mg_5AlSi_3AlO_{10}(OH)_8 + 14SiO_2 + 8H_2O(l) = 5Mg_6Si_4O_{10}(OH)_8 + 3Al_4\square_2Si_4O_{10}(OH)_8 \quad (2)$$

$$6Mg_5AlSi_3AlO_{10}(OH)_8 + 6KAlSi_3O_8 + 2SiO_2 + 2H_2O(l) = 5Mg_6Si_4O_{10}(OH)_8 + 6KAl_2Si_3AlO_{10}(OH)_2 \quad (3)$$

In the present study, Mn was regarded as equivalent to Mg following Walshe (1986). Equations 2 and 3 are the reactions forming the chlorite + quartz and chlorite + K-feldspar + illite + quartz assemblages in equilibrium with fluid, respectively.

The logarithms of the equilibrium constants, K, for equations 2 and 3 are

$$\log \mathrm{K}_{(2)} = -\frac{\Delta G^0_{\mathrm{r}(2)}}{2.303\mathrm{R}T} = \log\frac{a^5_{\mathrm{C1}}a^3_{\mathrm{C5}}}{a^6_{\mathrm{C2}}} - 14\log a_{\mathrm{qz}} - 8\log a_{\mathrm{water}} \quad (4)$$

$$\log \mathrm{K}_{(3)} = -\frac{\Delta G^0_{\mathrm{r}(3)}}{2.303\mathrm{R}T} = \log\frac{a^5_{\mathrm{C1}}}{a^6_{\mathrm{C2}}} + 6\log a_{\mathrm{illite}} - 6\log a_{\mathrm{K\text{-}spar}} - 2\log a_{\mathrm{qz}} - 2\log a_{\mathrm{water}} \quad (5)$$

where $\Delta G^o_{\mathrm{r(i)}}$ is the standard free energy change of reaction i at T and P, R is the gas constant, a_{Ci} and a_j are the activities of C_i component in chlorite solid solution and j phase, respectively. Assuming that $a_{\mathrm{qz}} = a_{\mathrm{K\text{-}spar}} = a_{\mathrm{illite}} = a_{\mathrm{water}} = 1$, equations 4 and 5 are written as

$$\log \mathrm{K}_{(2)} = 5 \log a_{\mathrm{C1}} + 3 \log a_{\mathrm{C5}} - 6 \log a_{\mathrm{C2}} \quad (6)$$

$$\log \mathrm{K}_{(3)} = 5 \log a_{\mathrm{C1}} - 6 \log a_{\mathrm{C2}} \quad (7)$$

If the effect of pressure can be ignored and the change in heat capacity, ΔCp, of reactions 2 and 3 is assumed to be zero, the following relation may be established between the equilibrium constant of reaction and temperature:

$$\log \mathrm{K} = \frac{\mathrm{A}}{T} + \mathrm{B} \quad (8)$$

where T is the temperature in Kelvin and A and B are constants. Based on equation 8, Walshe (1986)

Table 1. Three models for ideal activities of chlorite solid-solution components used in the calculations of the geothermometer.

Component (abbreviation)	Chemical formula (half formula unit)	Ideal activity
Walshe (1986) model		
C1: Al-free chlorite (Afch)	$[Mg_6][Si_4]O_{10}(OH)_8$	$a1 = \mathrm{k1}(X_{\mathrm{Mg,\,oct}})^6(X_{\mathrm{Si,\,tet}})^2$
C2: Clinochlore (Clin)	$[Mg_5Al][Si_3Al]O_{10}(OH)_8$	$a2 = \mathrm{k2}(X_{\mathrm{Mg,\,oct}})^5(X_{\mathrm{Al,\,oct}})(X_{\mathrm{Si,\,tet}})(X_{\mathrm{Al,\,tet}})$
C3: Chamosite (Chm)	$[Fe^{2+}_5Al][Si_3Al]O_{10}(OH)_8$	$a3 = \mathrm{k3}(X_{\mathrm{Fe,\,oct}})^5(X_{\mathrm{Al,\,oct}})(X_{\mathrm{Si,\,tet}})(X_{\mathrm{Al,\,tet}})$
C5: Pyrophyllite-gibbsite (Pyp)	$[Al_4\square_2][Si_4]O_{10}(OH)_8$	$a5 = \mathrm{k5}(X_{\square,\,\mathrm{oct}})^2(X_{\mathrm{Al,\,oct}})^4(X_{\mathrm{Si,\,tet}})^2$
		where k1 = 1; k2 = 59.720 = k3; k5 = 45.563
Vidal *et al*. (2001) model		
C1: Clinochore (Clin)	$[Mg_5Al][Si_3Al]O_{10}(OH)_8$	$a1 = \mathrm{k1}(X_{\mathrm{Mg},\,M1})(X_{\mathrm{Mg},\,M2+M3})^4(X_{\mathrm{Si,\,T2}})(X_{\mathrm{Al,T2}})$
C2: Chamosite (Chm)	$[Fe^{2+}_5Al][Si_3Al]O_{10}(OH)_8$	$a2 = \mathrm{k2}(\mathrm{X_{Fe,\,M1}})(\mathrm{X}_{\mathrm{Fe},\,M2+M3})^4(X_{\mathrm{Si,\,T2}})(X_{\mathrm{Al,\,T2}})$
C3: Sudoite (Sud)	$[Mg_2Al_3\square][Si_3Al]O_{10}(OH)_8$	$a3 = \mathrm{k3}(X_{\square,\,M1})(X_{\mathrm{Al},\,M2+M3})^2(X_{\mathrm{Mg},\,M2+M3})^2(X_{\mathrm{Si},\,T2})(X_{\mathrm{Al},\,T2})$
C4: Corundophilite (Crdp)	$[Mg_4Al_2][Si_2Al_2]O_{10}(OH)_8$	$a4 = \mathrm{k4}(X_{\mathrm{Al},\,M1})(X_{\mathrm{Mg},\,M2+M3})^4(X_{\mathrm{Al},\,T2})^2$
		where k1 = 4 = k2; k3 = 64; k4 = 1
This study model		
C1: Al-free chlorite (Afch)	$[Mg_6][Si_4]O_{10}(OH)_8$	same as *a*1 of Walshe (1986) model
C2: Corundophilite (Crdp)	$[Mg_4Al_2][Si_2Al_2]O_{10}(OH)_8$	$a2 = \mathrm{k2}(\mathrm{X_{Mg,\,oct}})^4(\mathrm{X_{Al,\,oct}})^2(\mathrm{X_{Al,\,tet}})^2$
C3: Chamosite (Chm)	$[Fe^{2+}_5Al][Si_3Al]O_{10}(OH)_8$	same as *a*3 of Walshe (1986) model
C4: Sudoite (Sud)	$[Mg_2Al_3\square][Si_3Al]O_{10}(OH)_8$	$a4 = \mathrm{k4}(X_{\mathrm{Mg,\,oct}})^2(X_{\mathrm{Al,\,oct}})^3(X_{\square,\,\mathrm{oct}})(\mathrm{X_{Si,\,tet}})(\mathrm{X_{Al,\,tet}})$
		where k2 = 45.563; k4 = 1728

Note: $X_{j,s}$ is the mole fraction of the j cation on the s site and $\mathrm{k_i}$ is a normalization factor.

calibrated the thermodynamic properties of the end-member components from equations 2 and 3, using the composition data of natural chlorite and the measured temperatures from active and fossil geothermal systems and assuming an ideal solid solution model for chlorite in which the activities of equations 6 and 7 can be approximated by the ideal activities given in Table 1. Finally he gave the following two geothermometers:

$$T(^{\circ}\mathrm{C}) = \frac{1626}{6.542 + \frac{1}{3}\log \mathrm{K}_{(2)}} - 273 \qquad (9)$$

for reaction 2, and

$$T(^{\circ}\mathrm{C}) = \frac{1113}{0.575 + \frac{1}{6}\log \mathrm{K}_{(3)}} - 273 \qquad (10)$$

for reaction 3. Walshe (1986) added another assumption in his actual calculations of the geothermometer as $a_{\text{pyrophyllite-gibbsite}} = X_{\text{pyrophyllite-gibbsite}}$, where X is the mole fraction of the pyrophyllite-gibbsite component.

Using the geothermometer in equation 9 applied to a chlorite + quartz assemblage, the formation temperatures of the Niger, Rouez, and Saint Martin chlorites were estimated assuming three different cases: (Case 1) all Fe is considered as Fe(II); (Case 2) all Fe(III) is located in the octahedral sites where it substitutes for $^{\mathrm{VI}}$Al; (Case 3) Fe(III) equally replaces both $^{\mathrm{VI}}$Al and $^{\mathrm{IV}}$Al. The results are plotted as the relationship between the estimated temperature and the $^{\mathrm{IV}}$Al content based on O = 28 (Figure 3). The different assumptions established in the structural formula calculations clearly influence the estimated temperatures of chlorite formation. Case 1 provides the greatest temperature estimates which range from 199 to 516ºC for Rouez, 112–204ºC for Niger, and 186–353ºC for Saint Martin chlorites. These temperatures contain many values inconsistent with the expected temperatures from observations in nature, though these expected temperatures are broadly estimated values. In the calculations used for the conditions in Cases 2 and 3, the amount of Fe(III) was determined independently using Mössbauer spectroscopic analysis and was cast into the octahedral and/or tetrahedral sites following the calculation procedure of Walshe (1986). Calculations using the conditions in Cases 2 or 3 gave a temperature range of 182–283ºC or 168–278ºC, 107–186ºC or 85–168ºC, and 153–240ºC or 146–238ºC for Rouez, Niger, and Saint Martin chlorites, respectively. Though the two cases gave similar sets of values, the Case 3 temperatures are slightly underestimated by ~10–20ºC in comparison with those of Case 2. Though a positive correlation was found between the formation temperature and the $^{\mathrm{IV}}$Al content, regardless of the assumption used in the calculations, the relationship is not consistent with the empirical calibration curves proposed by Cathelineau (1988) and Hillier and Velde (1991).

As mentioned previously, the mineral assemblages of Rouez and Saint Martin are similar to that formed in propylitic alteration, *i.e.* albite + epidote + chlorite + illite ± K-feldspar (Meyer and Hemley, 1967). The results obtained using the geothermometer from equation 10, applicable to reaction 3 containing K-feldspar and illite, gave a negative correlation

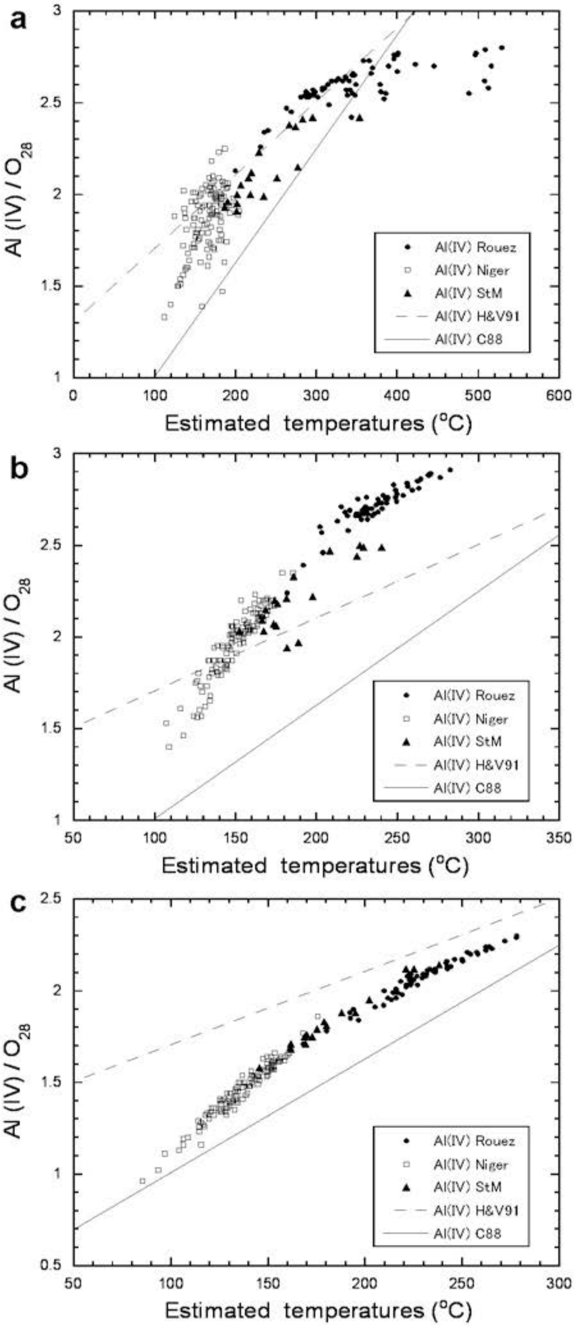

Figure 3. Plots of tetrahedral Al contents and estimated temperatures using Walshe's geothermometer of equation 9 in (a) Case 1, (b) Case 2, and (c) Case 3. The solid and dashed curves are the empirical calibrations proposed by Cathelineau (1988) (C88) and Hillier and Velde (1991) (H&V91), respectively.

between the ^{IV}Al content and temperature for the Rouez and Saint Martin chlorites. Consequently, equation 10 was not used as a geothermometer for low-T chlorites.

Vidal et al. (2001) geothermometer

Similar to Walshe (1986), Vidal *et al.* (2001) described the formation of the chlorite + quartz assemblage by the following reaction:

$$2Mg_5AlSi_3AlO_{10}(OH)_8 + 3Mg_2Al_3\square Si_3AlO_{10}(OH)_8 = 4Mg_4Al_2Si_2Al_2O_{10}(OH)_8 + 7SiO_2 + 4H_2O(l) \quad (11)$$

The equilibrium constant of reaction 11 is expressed by:

$$\log K_{(11)} = -\frac{\Delta G^0_{r(11)}}{2.303RT} = \log\left[\frac{a^4_{crdp}}{a^2_{clin}a^3_{sud}}\right]_{ideal} + \log\left[\frac{\gamma^4_{crdp}}{\gamma^2_{clin}\gamma^3_{sud}}\right]_{non\text{-}ideal} \quad (12)$$

assuming $a_{qz} = a_{water} = 1$. The γ_i is the activity coefficient of component i. The ideal activity part of equation 12 may be approximated as a function of temperature in a narrow range of pressure (*e.g.* vapor-saturation pressures of liquid water at temperatures) as follows:

$$\log K'_{(11)} = \log\left[\frac{a^4_{crdp}}{a^2_{clin}a^3_{sud}}\right]_{ideal} = \frac{A}{T} + B \quad (13)$$

The relationship between $1/T$ and the logarithmic ideal activities product of equation 13 was plotted (Figure 4) using the estimated formation temperature and chlorite composition in the chlorite + quartz assemblage given in the appendix (p. 589) of Vidal *et al.* (2001). From the regression of plots, the following geothermometer for the chlorite + quartz assemblage was obtained:

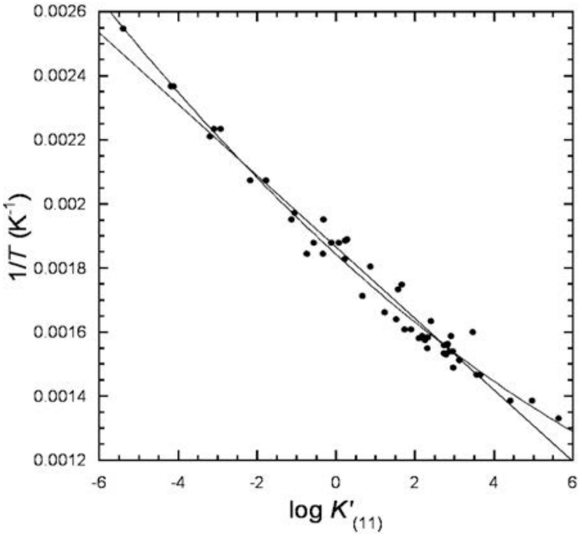

Figure 4. Relationship between $1/T$ and log $K'_{(11)}$ of the chemical compositions and estimated temperatures for the chlorite + quartz assemblages listed in the appendix of Vidal *et al.* (2001). Two regression curves correspond to the linear form of equation 14 and quadratic equation 15, respectively. See the details in the text.

$$T(^\circ C) = \frac{1}{0.00187 - 1.114 \times 10^{-4}x} - 273 \quad (r^2 = 0.970) \quad (14)$$

where

$$x = \log K'_{(11)} = 4\log a^{ideal}_{crdp} - 2\log a^{ideal}_{clin} - 3\log a^{ideal}_{sud}$$

From a statistical point of view, the quadratic equation gave a reasonably good fit:

$$T(^\circ C) = \frac{1}{0.00184 - 1.113 \times 10^{-4}x + 3.407 \times 10^{-6}x^2} - 273 \quad (r^2 = 0.978) \quad (15)$$

where r^2 is the square of the correlation coefficient r.

Vidal's geothermometry cannot be applied to chlorites with Si>3 p.h.f.u. (O = 14) because of the primary assumption. Thus, excluding chlorite data where Si>3 p.h.f.u., the formation temperatures of Rouez, Niger, and Saint Martin chlorites were estimated only for the conditions in Cases 1 and 2 (Figure 5). Using Vidal's geothermometer, calculating the formation temperatures was impossible for Case 3 conditions in which Fe(III) was cast into the tetrahedral and octahedral sites. The estimated temperatures of formation in Case 1 conditions are 150−747ºC, 21−488ºC, and 85−639ºC for Rouez, Niger, and Saint Martin chlorites, respectively. The respective maximum values of the estimated temperatures are considerably higher than those estimated using Walshe's geothermometer (equation 9); they are also inconsistent with observations in nature. Calculations using Case 2 conditions gave temperature ranges of 146−367ºC, 36−216ºC, and 105−349ºC for Rouez, Niger, and Saint Martin chlorites, respectively. As shown in Figure 5, Vidal's geothermometer shows a positive correlation between the temperature and ^{IV}Al content, but, regardless of the assumptions used in the calculations, the relationship is not consistent with the empirical calibration curves proposed by Cathelineau (1988) and Hillier and Velde (1991). Each sample seems to give a particular trend.

New geothermometer

The calibrated thermodynamic properties of the end-member components and the resulting estimated formation temperatures of Vidal *et al.* (2001) were assumed to be correct. A semi-empirical geothermometer based on four new end-member components: corundophilite, chamosite, sudoite, and Al-free chlorite was constructed,

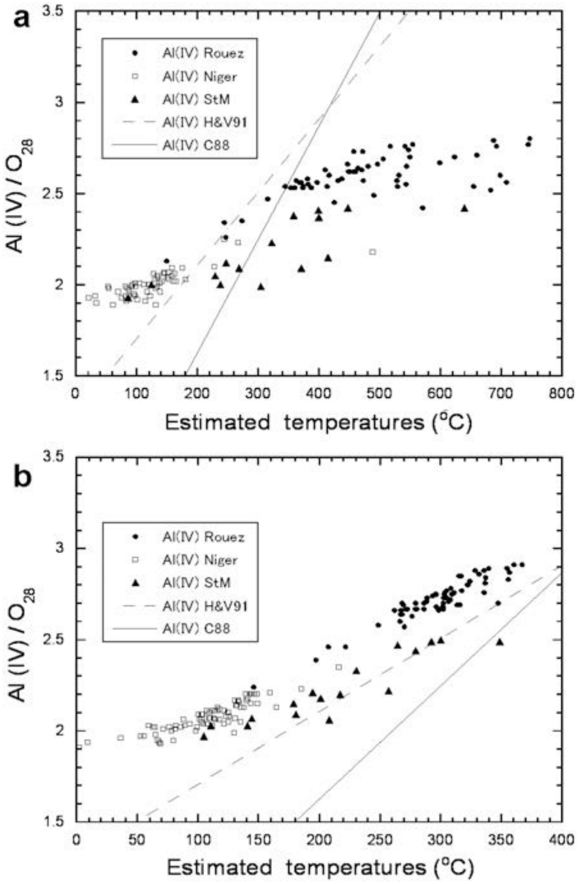

Figure 5. Plots of tetrahedral Al contents and estimated temperatures using Vidal's geothermometer of equation 15 in (a) Case 1 and (b) Case 2. The solid and dashed curves are the empirical calibrations proposed by Cathelineau (1988) (C88) and Hillier and Velde (1991) (H&V91), respectively.

taking into account the compositional variations of low-*T* chlorite (Figure 2). The reaction of formation of the chlorite + quartz assemblage is as follows:

$$3Mg_2Al_3\square Si_3AlO_{10}(OH)_8 + Mg_6Si_4O_{10}(OH)_8 = 3Mg_4Al_2Si_2Al_2O_{10}(OH)_8 + 7SiO_2 + 4H_2O\ (l) \quad (16)$$

Assuming the ordering of Si and Al in tetrahedral sites but a random mixing in a single type of octahedral site and using the ideal activities given in Table 1, the temperature data given by Vidal *et al*. (2001), which are the same as those used in Figure 4, were plotted *vs.* the logarithmic ideal activity product of reaction 16. The new geothermometer is obtained as follows:

$$T(^\circ\mathrm{C}) = \frac{1}{0.00264 - 2.897 \times 10^{-4}x} - 273 \qquad (r^2 = 0.773) \quad (17)$$

where

$$x = \log K'_{(16)} = 3\log a^{\mathrm{ideal}}_{\mathrm{crdp}} - 3\log a^{\mathrm{ideal}}_{\mathrm{sud}} - \log a^{\mathrm{ideal}}_{\mathrm{Afch}}$$

The following quadratic equation also gave a good fit from a statistical point of view:

$$T(^\circ\mathrm{C}) = \frac{1}{0.00293 - 5.13 \times 10^{-4}x + 3.904 \times 10^{-5}x^2} - 273 \qquad (r^2 = 0.786) \quad (18)$$

Here, $a_{\mathrm{qz}} = a_{\mathrm{water}} = 1$ was also assumed. Using equation 18, the formation temperatures of Niger, Rouez, and Saint Martin chlorites can also be estimated using the conditions in Cases 1–3 (Figure 6). In Case 1 conditions (where all Fe is ferrous), the estimated temperatures are 212–528°C, 59–277°C, and 335–519ºC for Rouez, Niger, and Saint Martin chlorites, respectively. They all are greater than those given by the Walshe geothermometer and equivalent to or less than those given by the Vidal *et al.* thermometer. In Case 2 conditions, the temperatures are 127–373ºC, 12–156ºC, and 192–349ºC for Rouez, Niger, and Saint Martin, respectively; estimated using Case 3 conditions and are smaller by ~30–50ºC. Again, using the present geothermometer, *T* and $^{\mathrm{IV}}$Al were clearly positively correlated but, whatever the assumption used in the calculations, the correlation was different from that obtained using the empirical calibration curves proposed by Cathelineau (1988) and Hillier and Velde (1991).

COMPARISON OF THE THREE GEOTHERMOMETERS

An assumption of $a_{\mathrm{water}} = 1$ has been established in the derivation of the three geothermometers. The condition of $a_{\mathrm{water}} < 1$, from equations 2, 11, and 16, will result in much larger underestimates of the temperature of chlorite formation in the Walshe geothermometer, and larger overestimates in the Vidal *et al.* and present geothermometers, regardless of other calculation conditions. Although the actual activity values of water are unknown in the cases of Niger, Rouez, and Saint Martin, the assumption of $a_{\mathrm{water}} = 1$ is generally reasonable in diagenetic to low-grade metamorphic and hydrothermal environments related to the chlorite formation.

The calculation based on the assumption that all iron is Fe(II) (Case 1) led to a considerable overestimate of the formation temperature regardless of the geothermometer used. The low-*T* chlorites studied here have appreciable amounts of Fe(III), at least 14% of the total Fe. These values are significantly greater than those of common metamorphic chlorites (Foster, 1962), emphasizing the necessity of correcting for the Fe(III) content as precisely as possible before estimating the formation temperature, as exemplified by the studies of metamorphic chlorites by Vidal *et al*. (2005, 2006). The Case 3 calculation (Fe(III) is cast equally into both the tetrahedral and octahedral sites) provides the smallest formation-temperature estimates using the Walshe and present models (Figures 3, 6). However, none of the Mössbauer spectroscopic data used here support the presence of tetrahedral Fe(III) in the chlorite samples studied; consequently the assumption that all Fe(III) occupies only the octahedral sites (Case 2) is the most reasonable one at present for estimating the formation temperatures of Fe(III)-bearing, low-*T* chlorites.

The formation temperatures, calculated using Case 2 conditions, were compared (Figure 7) for each of the three geothermometers, for the Niger, Rouez, and Saint

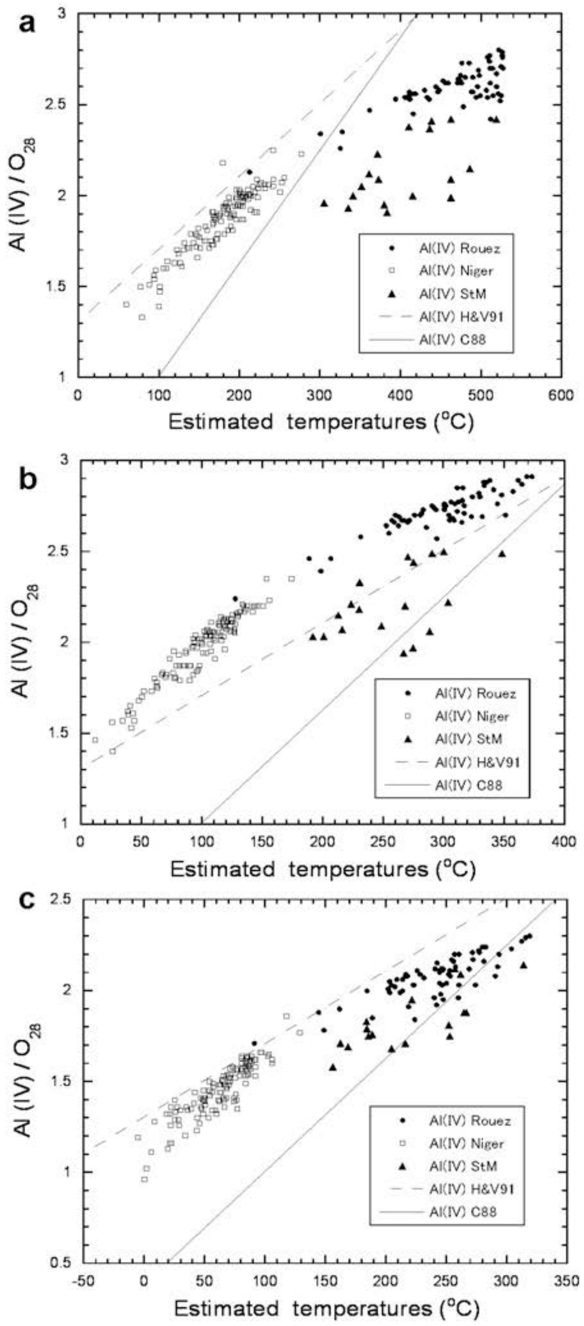

Figure 6. Plots of tetrahedral Al contents and estimated temperatures using the new geothermometer of equation 18 in (a) Case 1, (b) Case 2, and (c) Case 3. The solid and dashed curves are the empirical calibrations proposed by Cathelineau (1988) (C88) and Hillier and Velde (1991) (H&V91), respectively.

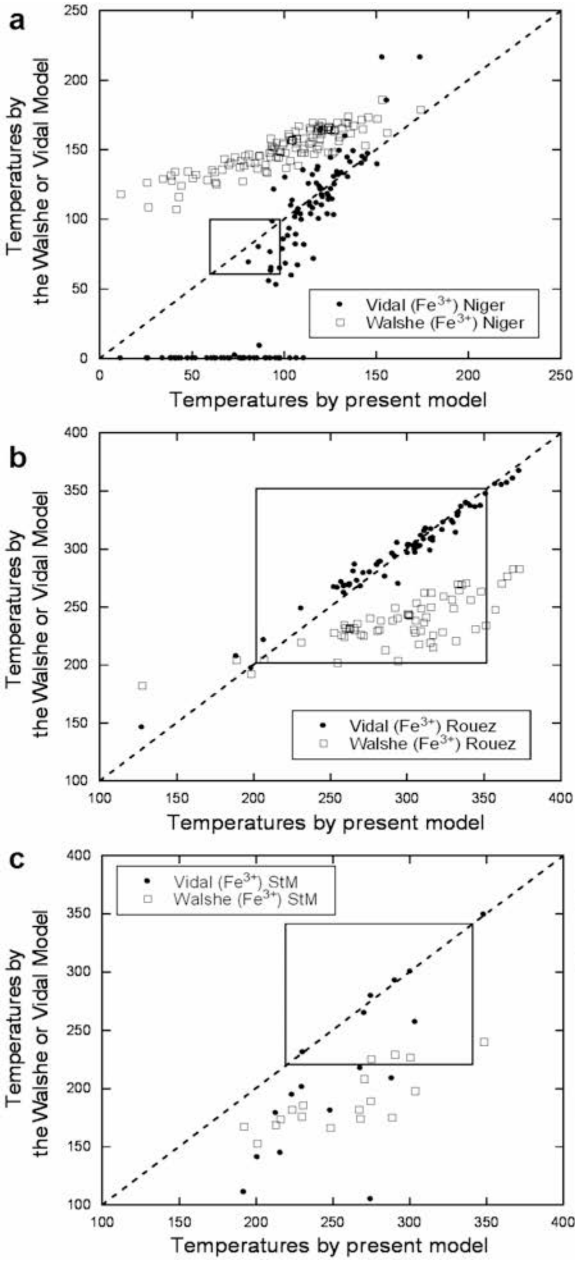

Figure 7. Comparison of estimated temperatures for the formation of chlorites in Case 2 conditions using three geothermometers: (a) Niger, (b) Rouez, and (c) Saint Martin. Solid circles and open squares are temperatures from the Walshe and Vidal geothermometers, respectively. Large square areas correspond to the expected temperatures of natural observations in the three fields.

Martin chlorites. For the Niger chlorites that formed at the lowest temperatures (probably 80±20ºC), the Walshe geothermometer gave larger overestimates, as a whole, compared to the Vidal and present geothermometer. Many of the data (>40% of the analyses) were eliminated from the calculations using the Vidal *et al.* geothermometer (plotted as zero in the figure) because its application is restricted to compositions of Si < 3 p.h.f.u. For Rouez and Saint Martin chlorites, which formed at greater temperatures, estimates given by the three geothermometers are within the expected values of the formation temperature. However, the Walshe geothermometer systematically seems to give values which are slightly smaller than those provided by the present geothermometer. Interestingly, the estimate by the Vidal *et al.* geothermometer shows systematic deviation toward smaller temperatures for chlorites from alteration zones 2 and 3 of Saint Martin, which have greater proportions of Fe(III). The difference in the estimated temperatures given by the three geothermometers is due to the choice of different end members and calculation of activities as well as the differences in the thermodynamic properties used in the calculations, as mentioned above. In short, comparison of three geothermometers indicates that the present geothermometer, based on a random-mixing, solid-solution model, performs well when estimating the temperature of formation of low-*T* chlorite with a wide range of compositional variations along with variable Fe(III) contents.

As for the peculiar compositional variations of low-*T* chlorites, Hillier and Velde (1992) and Hillier (1994) pointed out the possibility that the compositional variation feature in low-*T* chlorites is partly ascribed to the contamination of kaolinite, or the interstratification with berthierine or smectite. The influence of interstratification with smectite is negligible here because only analyses with <0.5 wt.% total $Na_2O + CaO + K_2O$ were selected in this study. Contamination by kaolinite and/or quartz will result in the extremely low estimates of temperature of chlorite formation in the present geothermometric calculation. This may well be the case for some data from Niger chlorites which may be interstratified with berthierine. Interstratification and intergrowths in the chlorite–berthierine series are common phenomena in low-*T* chlorites (Xu and Veblen, 1996). However, in case of the interstratification with berthierine, distinguishing the compositions of interstratified phases from those of a solid-solution mineral is difficult using electron microprobe analysis. Patrier *et al.* (1991) indicated, in their Mössbauer study of epidote associated with chlorite from Saint Martin, that epidote crystallized at greater temperatures (>300ºC) displayed an equilibrium ordered-site distribution of Fe(III), whereas the non-equilibrium ordering state of epidote increased with decreasing formation temperature. Although the relationship between ordered-site occupancy in chlorite and temperature is unknown, rapid crystallization at lower temperatures is likely, leading to metastable disordered-site occupation, even in chlorite. This metastability may be a cause of the deviation toward smaller temperatures for chlorites from alteration zones 2 and 3 of Saint Martin in the calculation by the Vidal *et al.* geothermometer (Figure 7).

The relationship between the octahedral vacancies based on O = 28 and the estimated temperatures calculated using the present geothermometer in Case 2 conditions (Figure 8) illustrated that the numbers of vacancies decrease exponentially with increasing temperature from $\square = 2$ at low temperatures to almost negligible at temperatures of >400ºC. This $\square = 2$ value is equal to the vacancy composition of sudoite. The figure also indicates that the decreasing rate in number of vacancies with increasing temperature is sensitive to the Fe content of chlorite; it is smaller in Fe-rich than in Fe-poor chlorites. Finally, in spite of the fact that no detailed information on the ordering in terms of the cation substitution of low-*T* chlorites is available at present, the ordered-site substitution model applied to higher-grade metamorphic chlorites likely is not suitable for low-*T* chlorite solid solution. The octahedral cations in low-*T* chlorites may be randomly distributed among the *M* sites together with the vacancies, which may be a metastable state. With increasing temperature, the composition and structure of chlorite are changed according to the gradual decrease in the Si$\square R^{2+}_{-2}$

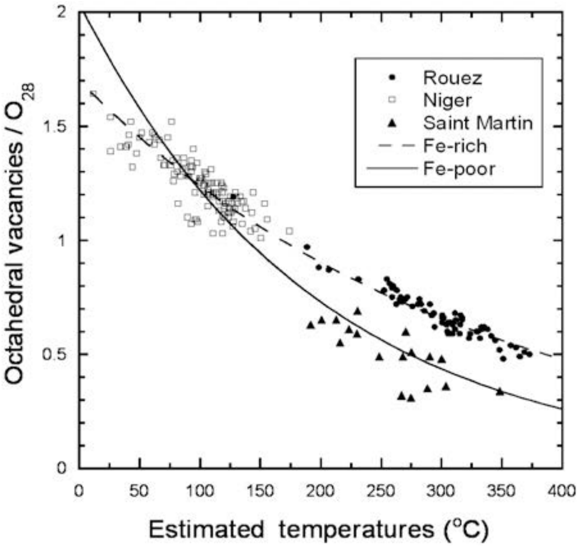

Figure 8. Relationship between the numbers of octahedral vacancies and estimated temperatures using the present geothermometer (equation 18) in Case 2 conditions. Squares, circles, and triangles represent chlorites from Niger, Rouez, and Saint Martin, respectively. The solid and dashed curves are regression curves for Fe-poor samples and Fe-rich samples, respectively.

substitution and the concomitant ordered-site occupation of octahedral cations and vacancies at a constant R^{3+} condition. When chlorite experiences a reduction of Fe(III) to Fe(II) with increasing temperature, the compositional variation is dominated by the Tschermak substitution.

SUMMARY AND CONCLUSIONS

The applicability of the geothermometers developed by Walshe (1986) and Vidal *et al.* (2001) was tested for low-*T* chlorites formed in diagenetic to very low-grade metamorphic environments. Results revealed that a preliminary determination of Fe(III) content is essential in estimating the temperature of formation of those chlorites. The compositional variations in low-*T* chlorites are generally characterized by greater Si contents and numbers of octahedral vacancies, and smaller Fe+Mg contents compared to higher-grade metamorphic chlorites. The vacancies are usually <1 p.h.f.u. based on O = 14. Such properties allow the proposal of a more convenient geothermometer which is different from that based on the ordered-site substitution model of cations and vacancies for higher-grade metamorphic chlorites. Instead, four end-member components are used as the basis: Al-free trioctahedral chlorite, corundophilite, chamosite, and sudoite, together with the assumption that octahedral cations and vacancies are randomly distributed in the *M* sites. The newly proposed geothermometer provides temperature estimates consistent with petrographic observations for chlorites formed at lower temperatures after correcting the Fe(III) content. With increasing temperature, chlorite tends to have a more ordered site-occupancy structure. Concomitantly, the bulk composition is controlled by the $\mathrm{Si}\square R^{2+}_{-2}$ exchange at lower-temperature conditions while it is controlled by the Tschermak exchange at greater temperatures. Unfortunately, no detailed information is available regarding cation ordering distribution in the structural sites of low-*T* chlorites. Though dependent on the primary Fe(III) content and secondary oxidation, the geothermometer developed by Vidal *et al.* (2001) may be suitable for estimating the temperature of formation of ordered chlorites, whereas the present geothermometer may be applicable to disordered chlorites formed in diagenetic to very low-grade metamorphic environments. The transition temperature between disordered and ordered chlorites may be ~250ºC, from the data obtained in the present study.

ACKNOWLEDGMENTS

A. Inoue is grateful to the Université de Poitiers for providing an opportunity to collaborate on this work. The authors are also grateful to Bruce Velde for stimulating discussion in the course of this work. Reviews by Olivier Vidal, Steve Hillier, and Bruno Lanson led to substantial improvements of the paper.

REFERENCES

Bailey, S.W. (1988) Chlorites: Structures and crystal chemistry. Pp. 347–403 in: *Hydrous Phyllosilicates (Exclusive of Micas)* (S.W. Bailey, editor). Reviews in Mineralogy, **19**, Mineralogical Society of America, Washington, D.C.

Baker, J. and Holland, T.J.B. (1996) Experimental reversals of chlorite compositions in divariant MgO-Al_2O_3-SiO_2-H_2O assemblages: implications for order-disorder in chlorites. *American Mineralogist*, **81**, 676–684.

Beaufort, D. (1986) Defenition des equilibres chlorite-mica blanc dans la metamorphisme et la metasomatisme: etude des metasediments encaisant l'amas sulfure de Rouez. PhD thesis, Universite de Poitiers, France.

Beaufort, D. (1987) Interstratified chlorite/smectite ('metamorphic vermiculite') in the Upper Precambrian greywackes of Rouez, Sarthe, France. *Proceedings of the International Clay Conference, Denver, 1985*, 59–65.

Beaufort, D., Westercamp, D., Legendre, O., and Meunier, A. (1990) The fossil hydrothermal system of Saint Martin: (1) Geology and lateral distribution of alterations. *Journal of Volcanology and Geothermal Research*, **40**, 219–243.

Beaufort, D., Patrier, P., Meunier, A., and Ottaviani, M.M. (1992) Chemical variations in assemblages including epidote and/or chlorite in the fossil hydrothermal system of Saint Martin (Lesser Antilles). *Journal of Volcanology and Geothermal Research*, **51**, 95–114.

Berman, R.G. (1988) Internally-consistent thermodynamic data for minerals in the system Na_2O-K_2O-CaO-MgO-FeO-Fe_2O_3-Al_2O_3-SiO_2-TiO_2-H_2O-CO_2. *Journal of Petrology*, **29**, 445–522.

Cathelineau, M. (1988) Cation site occupancy in chlorites and illites as a function of temperature. *Clay Minerals*, **23**, 471–485.

Curtis, C.D., Hughes, C.R., Whiteman, J.A., and Whittle, C.K. (1985) Compositional variation within some sedimentary chlorites and some comments on their origin. *Mineralogical Magazine*, **49**, 375–386.

De Caritat, P., Hutcheon, I., and Walshe, J.L. (1993) Chlorite geothermometry: A review. *Clays and Clay Minerals*, **41**, 219–239.

Foster, M.D. (1962) Interpretation of the composition and a classification of the chlorites. *U.S. Geological Survey Professional Paper*, 414-A, 33 pp.

Hayes, J.B. (1970) Polytypism of chlorite in sedimentary rocks. *Clays and Clay Minerals*, **18**, 285–306.

Helgeson, H.C., Delany, J.M., Nesbitt, H.W., and Bird, D.K. (1978) Summary and critique of the thermodynamic properties of rock-forming minerals. *American Journal of Science*, **278-A**, 229 pp.

Hillier, S. (1994) Pore-lining chlorites in siliciclastic reservoir sandstones: electron microprobe, SEM and XRD data, and implications for their origin. *Clay Minerals*, **29**, 665–679.

Hillier, S. and Velde, B. (1991) Octahedral occupancy and the chemical composition of diagenetic (low-temperature) chlorites. *Clay Minerals*, **26**, 149–168.

Hillier, S. and Velde, B. (1992) Chlorite interstratified with a 7 Å mineral: An example from offshore Norway and possible implications for the interpretation of the composition of diagenetic chlorites. *Clay Minerals*, **27**, 475–486.

Holland, T.J.B. and Powell, R. (1998) An internally consistent thermodynamic data set for phases of petrological interest. *Journal of Metamorphic Geology*, **16**, 309–343.

Holland, T.J.B., Baker, J., and Powell, R. (1998) Mixing properties and activity-composition relationships of chlorites in the system MgO-FeO-Al_2O_3-SiO_2-H_2O. *European Journal of Mineralogy*, **10**, 395–406.

Hutcheon, I. (1990) Clay-carbonate reactions in the Venture area, Scotia Shelf, Nova Scotia, Canada. Pp. 199–212 in:

Fluid-Mineral Interactions: A Tribute to H.P. Eugster (R.J. Spencer and I.-M. Chou, editors). Geochemical Society Special Publication 2.

Laird, J. (1988) Chlorites: Metamorphic petrology. Pp. 405−453 in: *Hydrous Phyllosilicates (Exclusive of micas)* (S.W. Bailey, editor). Reviews in Mineralogy, **19**, Mineralogical Society of America, Washington, D.C.

Meyer, C. and Hemley, J.J. (1967) Wall rock alteration. Pp. 166−235 in: *Geochemistry of Hydrothermal Ore Deposits* (H.L. Barnes, editor). Holt, Rinehart and Winston, New York.

Newman, A.C.D. and Brown, G. (1987) The chemical constitution of clays. Pp. 1−128 in: *Chemistry of Clays and Clay Minerals* (A.C.D. Newman, editor). Monograph **6**, Mineralogical Society, London.

Parra, T., Vidal, O., and Theye, T. (2005) Experimental data on the Tschermak substitution in Fe-chlorite. *American Mineralogist*, **90**, 359−370.

Patrier, P., Beaufort, D., Touchard, G., and Fouillac, A.M. (1990) Crystal side of epidotes: A potentially exploitable geothermometer in geothermal fields? *Geology*, **18**, 1126−1129.

Patrier, P., Beaufort, D., Meunier, A., Eymery, J-P., and Petit, S. (1991) Determination of the non-equilibrium ordering state in epidote from the ancient geothermal field of Saint Martin: Application of Mössbauer spectroscopy. *American Mineralogist*, **76**, 602−610.

Powell, R. (1978) *Equilibrium Thermodynamics in Petrology: An Introduction*. Harper & Row, London, 284 pp.

Saccocia, P.J. and Seyfried, W. (1994) The solubility of chlorite solid solutions in 3.2 wt.% NaCl fluids from 300−400ºC, 500 bars. *Geochimica et Cosmochimica Acta*, **58**, 567−585.

Vidal, O., Goffe, B., and Theye, T. (1992) Experimental study of the stability of sudoite and magnesiocarpholite and calculation of a new petrogenetic grid for the system FeO-MgO-Al_2O_3-SiO_2-H_2O. *Journal of Metamorphic Geology*, **10**, 603−614.

Vidal, O., Goffe, B., Parra, T., and Bousquet, R. (1999) Calibration and testing of an empirical chloritoid-chlorite Mg-Fe thermometer and thermodynamic data for daphnite. *Journal of Metamorphic Geology*, **17**, 25−39.

Vidal, O, Parra, T., and Trotet, F. (2001) A thermodynamic model for Fe-Mg aluminous chlorite using data from phase equilibrium experiments and natural pelitic assemblages in the 100º to 600ºC, 1 to 25 kb range. *American Journal of Science*, **301**, 557−592.

Vidal, O., Parra, T., and Vieillard, P. (2005) Thermodynamic properties of the Tschermak solid solution in Fe-chlorite; Application to natural examples and possible role of oxidation. *American Mineralogist*, **90**, 347−358.

Vidal, O., De Andrade, V., Lewin, E., Munoz, M., Parra, T., and Pascarell, S. (2006) P-T-deformation-Fe(III)/Fe(II) mapping at the thin section scale and comparison with XANES mapping: application to a garnet-bearing metapelite from the Sambagawa metamorphic belt (Japan). *Journal of Metamorphic Geology*, **24**, 669−683.

Walker, J.R. (1993) Chlorite polytype geothermometry. *Clays and Clay Minerals*, **41**, 260−267.

Walshe, J.L. (1986) A six-component chlorite solid solution model and the conditions of chlorite formation in hydrothermal and geothermal systems. *Economic Geology*, **81**, 681−703.

Walshe, J.L. and Solomon, M. (1981) An investigation into the environment of formation of the volcanic-hosted Mt. Lyell copper deposits using geology, mineralogy, stable isotopes, and a six-component chlorite solid solution model. *Economic Geology*, **76**, 246−284.

Wiewióra, A. and Weiss, Z. (1990) Crystallochemical classifications of phyllosilicates based on the unified system of projection of chemical composition: II The chlorite group. *Clay Minerals*, **25**, 83−92.

Xu, H. and Veblen, D.R. (1996) Interstratification and other reaction microstructures in the chlorite-berthierine series. *Contributions to Mineralogy and Petrology*, **124**, 291−301.

Zane, A., Sassi, R., and Guidotti, C.V. (1998) New data on metamorphic chlorite as a petrogenetic indicator mineral, with special regard to greenschist-facies rocks. *The Canadian Mineralogist*, **36**, 713−726.

(*Received 3 November 2008; revised 10 March 2009; Ms. 0163; A.E. B. Lanson*)